

Hunting for sterile neutrino with collider signatures

Hao Yang^{1*}, Bingwei Long^{1†} and Cong-Feng Qiao^{2,3‡}

¹ *College of Physics, Sichuan University, Chengdu, Sichuan 610065, China*

² *School of Physics, University of Chinese Academy of Sciences,
Yuquan Road 19A, Beijing 100049*

³ *CAS Key Laboratory of Vacuum Physics, Beijing 100049, China*

Abstract

We study the feasibility to observe sterile neutrino at the high energy colliders, using direct production channels $e^+e^- \rightarrow \bar{\nu}_e N$, $e^-\gamma \rightarrow NW^-$ and indirect production channels through heavy meson/baryon and Higgs decay. We thus cover a mass window that is between what can be studied in heavy hadron factories and high energy colliders. For $e^+e^- \rightarrow \bar{\nu}_e N$ channel, the sensitivity of active-sterile mixing $|U_{eN}|^2$ in the lower mass end ($0.3 \sim 2$ GeV) could be 10^{-6} at the SuperKEKB under its operation with designed luminosity, the sensitivity for hundreds GeV region can be further extended to 10^{-7} at the CEPC and the ILC. We also explore the heavy sterile neutrino production through $e^-\gamma \rightarrow NW^-$ channel at the ep collider, the mixing $|U_{eN}|^2$ is estimated to reach a sensitivity of 10^{-4} at the LHeC if m_N to be electroweak energy mass scale, which can shed light on sterile neutrino searching at this mass region. For heavy hadron decay, the lepton-number-violating process in $|\Delta L| = 2$ decays of $\Lambda_c, \Xi_c, \Xi_{cc}$ and Λ_b are explored via an intermediate on-shell Majorana neutrino in GeV scale. The branching fractions and the lower-limit on $|U_{\ell N}|^2$ versus m_N are given. The $Higgs \rightarrow W\mu\mu\pi$ channel is also considered, which is sensitive at lower mass scale.

* yanghao2023@scu.edu.cn

† bingwei@scu.edu.cn, corresponding author

‡ qiaocf@ucas.ac.cn, corresponding author

I. INTRODUCTION

The experimental observation of neutrino oscillation has conclusively shown small but non-zero neutrino mass. Since neutrinos are massless in the Standard Model (SM), the mass origin has become an important portal to physics beyond the standard model (BSM). There are generally three theoretical explanations: see-saw mechanism [1, 2], radiative generated mass [3] and extra-dimensions [4]. While originally the see-saw mechanism resort the smallness to the presence of extra field with far beyond electroweak energy mass scale. There are also models where extra fields are not so heavy [5], leaving the open possibility for eV to TeV scale extra sterile neutrinos, and hence feasible for collider searches. The reason for the smallness is yet not fully understood, but the very existence of neutrino mass may indicate the existence of a right-handed gauge-singlet (sterile) neutrino N_R . The Dirac or Majorana nature of N_R can be identified by neutrinoless double-beta decay $0\nu\beta\beta$ [6] of nucleus or other $W^{*,\pm}W^{*,\pm} \rightarrow \ell^\pm\ell^\pm$ induced processes, which led to Standard Model forbidden lepton number violation ($\Delta L = 2$) processes.

Various laboratory searches have put stringent constraints on sterile neutrino mixing with active ones in a broad mass range from eV to TeV. For the sterile neutrino mass below MeV, it is proposed to search kinks in the Kurie plots in the nuclear beta decays of ^{187}Re [7], ^3H [8], ^{63}Ni [9], ^{35}S [10], ^{20}F [11], *etc.* Analogously, search peaks in the energy spectra of two-body leptonic decays of charged pseudoscalar meson, *e.g.*, π [12], K [13], for heavier sterile neutrino mass from MeV to GeV. Sterile neutrino can be also tested via its effects on the lepton universality ratio $\text{BR}(M^+ \rightarrow \ell_1^+ \nu_{\ell_1})/\text{BR}(M^+ \rightarrow \ell_2^+ \nu_{\ell_2})$, $M = \pi, K, D, D_s$ [14, 15], from their SM values, or via Majorana neutrino induced lepton number violation (LNV) three/four body decay of heavy meson, *e.g.*, $D^+ \rightarrow \pi^-(K^-)e^+e^+$ at the CLEO [16], $B^+ \rightarrow D^- + \ell^+\ell'^+$ at the Belle [17], $B^- \rightarrow \pi^+\mu^-\mu^-$ at the LHCb [18], $D \rightarrow K\pi e^+e^+$ at the BESIII [19]. For the heavy sterile neutrino mass above GeV, using the possible production of sterile neutrino in the Z^0 boson decay $Z^0 \rightarrow \nu(\bar{\nu})N$, limits on the active-sterile mixing are obtained by L3 [20] and DELPHI [21], analogous production in the W boson decay $W \rightarrow \ell N$ is explored at the ATLAS

[22]. For the mass above electroweak energy mass scale, direct searches were performed employing same-sign dileptons plus jets [23–25], or $N \rightarrow \ell jj$ [26], $N \rightarrow \ell W$ [27] at the LHC.

Now in this article we give several complementary investigations to the previous work by studying the feasibility of collider test for sterile neutrino through: (1) direct production via e^+e^- , ep collision; (2) indirect production via heavy particles decay, *e.g.*, Higgs, heavy meson/baryon.

The rest of the paper is organized as follows. In Sec. II, we present the direct searches for sterile neutrino at the e^+e^- , ep colliders. In Sec. III, we investigate the indirect channels for sterile neutrino via heavy particle decay. The last section is reserved for summary and conclusions.

II. DIRECT PRODUCTION

A. e^+e^- collision

In the presence of one or several sterile neutrinos, active neutrinos in the flavor base are a mixture of the light and heavy sterile neutrinos in mass eigenstates. The lagrangian of interaction terms between sterile neutrino and gauge boson, Higgs boson in mass eigenstates are

$$\begin{aligned}
-\mathcal{L} = & \frac{g}{\sqrt{2}} W_\mu^+ \left(\sum_{\ell=e}^{\tau} \sum_{m=1}^3 U_{\ell m}^* \bar{\nu}_m \gamma_\mu P_L \ell + \sum_{\ell=e}^{\tau} \sum_{m'=4}^{3+n} V_{\ell m'}^* \bar{N}_{m'}^c \gamma_\mu P_L \ell \right) + h.c. \\
& + \frac{g}{2 \cos \theta_W} Z_\mu \left(\sum_{\ell=e}^{\tau} \sum_{m=1}^3 U_{\ell m}^* \bar{\nu}_m \gamma_\mu P_L \nu_\ell + \sum_{\ell=e}^{\tau} \sum_{m'=4}^{3+n} V_{\ell m'}^* \bar{N}_{m'}^c \gamma_\mu P_L \nu_\ell \right) + h.c., \\
& + \frac{g m_N}{2 m_W} H \sum_{\ell=e}^{\tau} V_{\ell N}^* \bar{N}^c P_L \nu_\ell + h.c., \tag{1}
\end{aligned}$$

where $g = \frac{e}{\sin \theta_W}$, θ_W is the weak Weinberg mixing angle and $\sin^2 \theta_W = 0.231$, $U_{\ell m}/V_{\ell m}$ is the Pontecorvo-Maki-Nakagawa-Sakata (PMNS) matrix [28, 29], charge conjugate state is defined as $\psi^c = \mathcal{C} \bar{\psi}^T$, the left hand projection operator $P_L = \frac{1 - \gamma^5}{2}$.

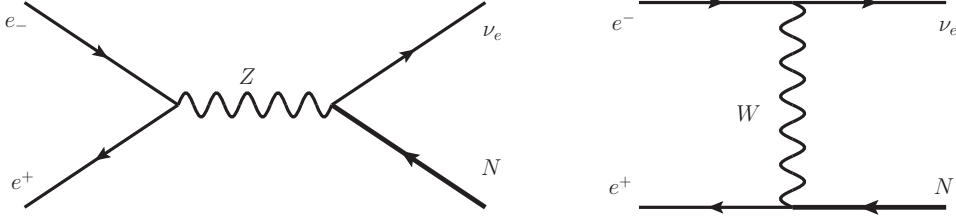


FIG. 1: Sterile neutrino production through Drell-Yan (Z) and W-exchange channels at the e^+e^- collider.

In this section we discuss the possible production of the sterile neutrino through e^+e^- collision, and its subsequent decay at the leading order. In this line, we address the dependency on active-sterile mixing $|U_{\ell N}|^2$ for the different colliders. There are two dominant production channels, one is an annihilation channel through Z boson (s-channel), another is given by the exchange of a W boson (t-channel), see FIG. 1. We note that the sterile neutrino can be also produced via e^+e^- annihilation into Higgs, which is largely suppressed by the tiny coupling between electron and Higgs.

In the previous researches, the $e^+e^- \rightarrow \nu N$ channel has been explored at various future high energy lepton colliders, see [30] for review. In this section, we study the sterile neutrino produced via s-channel and t-channel at the SuperKEKB, the Super Tau-Charm Facility (STCF), the Circular Electron Positron Collider (CEPC) and the International Linear Collider (ILC), where the final sterile neutrino is reconstructed by $\mu\pi$ -channel for light mass region and by ℓjj -channel for heavy mass region. Here and the rest of this article, one sterile neutrino N is supposed, one can easily extend our analysis to multi sterile neutrino model.

According to gauge-interaction lagrangian in (1), the canonical matrix element square takes the form:

$$\begin{aligned}
 |\mathcal{M}(e^+e^- \rightarrow \bar{\nu}_e N)|^2/|U_{eN}|^2 = & 8G_F^2 m_W^4 \left\{ \frac{4u(u - m_N^2)}{(m_W^2 - t)^2} - \frac{4(2s_w^2 - 1)u(m_N^2 - u)}{c_w^2 (m_W^2 - t)(m_Z^2 - s)} \right. \\
 & \left. + \frac{-m_N^2 [4s_w^4(t + u) + u(1 - 4s_w^2)] + 4s_w^4(t^2 + u^2) + u^2(1 - 4s_w^2)}{c_w^4 (m_Z^2 - s)^2} \right\},
 \end{aligned}
 \tag{2}$$

where G_F is the weak interaction Fermi constant with $G_F = \frac{\alpha\pi}{\sqrt{2}m_W^2 \sin^2\theta_W}$ is employed, the Mandelstam variables are define as $s = (p_{e^+} + p_{e^-})^2$, $t = (p_{e^-} - p_{\nu_e})^2$, $u = (p_{e^-} - p_N)^2$ with Mandelstam relation $s + t + u = m_N^2$, and $s_w = \sin\theta_W, c_w = \cos\theta_W, m_W = 80.377$ GeV, $m_Z = 91.187$ GeV. We have $|\mathcal{M}(e^+e^- \rightarrow \bar{\nu}_e N)|^2 = |\mathcal{M}(e^+e^- \rightarrow \nu_e \bar{N})|^2$ for the charge conjugated process.

The cross section is straightforward

$$\sigma(e^+e^- \rightarrow \bar{\nu}_e N) = \frac{1}{2} \frac{1}{2} \frac{1}{2s} \frac{1}{8\pi s} \int_{m_N^2-s}^0 |\mathcal{M}(e^+e^- \rightarrow \bar{\nu}_e N)|^2 dt, \quad (3)$$

where the first two $\frac{1}{2}$ are spin-polarization average factors of electron and positron, $\frac{1}{2s}$ and $\frac{1}{8\pi s}$ are the flux and two-body final state phase space factor.

TABLE I: The center-mass energy and integrated luminosity of current and future e^+e^- colliders. The integrated luminosity is estimated by $10^{34} \text{ cm}^{-2}\text{s}^{-1} \sim 1 \text{ ab}^{-1}/10$ years.

Collider	STCF	SuperKEKB	CEPC	ILC
$\sqrt{s}(\text{GeV})$	7	10.6	250	500
$\int d\mathcal{L}(\text{ab}^{-1})$	5	80	3	1.8

The direct search for sterile neutrino is considered at the future lepton colliders, the SuperKEKB, the STCF, the CEPC and the ILC, each with its own physics focus on bottom, tau-charm, Higgs and Z respectively. The center-mass energy and integrated luminosity after 10 years operation are listed in TABLE I. For the same strength of mixing parameter $U_{\ell N}$, the t-channel is enhanced approximately 1~2 magnitudes compared with the s-channel and hence get better sensitivity for $|U_{\ell N}|^2$. We noted that the s-channel can be largely enhanced at the Z-pole running for the CEPC and the ILC, the mainly contribution can be regarded as on-shell Z boson decay [21]. In our analysis, the sterile neutrino is reconstructed by $\mu\pi$ for light N, while for heavier N, the μjj -channel is adopted.

As estimated in [31, 32], the total decay width for Dirac sterile neutrino is set to be

$$\Gamma_N^{Dirac} = \begin{cases} 5 \sum_{\ell=e,\mu\tau} |U_{\ell N}|^2 \frac{G_F^2 m_N^5}{96\pi^3} & m_N < m_W \\ \sum_{\ell=e,\mu\tau} |U_{\ell N}|^2 \frac{3G_F m_N^3}{16\pi\sqrt{2}} & m_N > m_W, \end{cases} \quad (4)$$

here $U_{eN} = U_{\mu N} = U_{\tau N}$ is adopted for naturalness consideration. For Majorana sterile neutrino, $\Gamma_N^{Majorana} \approx 2\Gamma_N^{Dirac}$ is proposed.

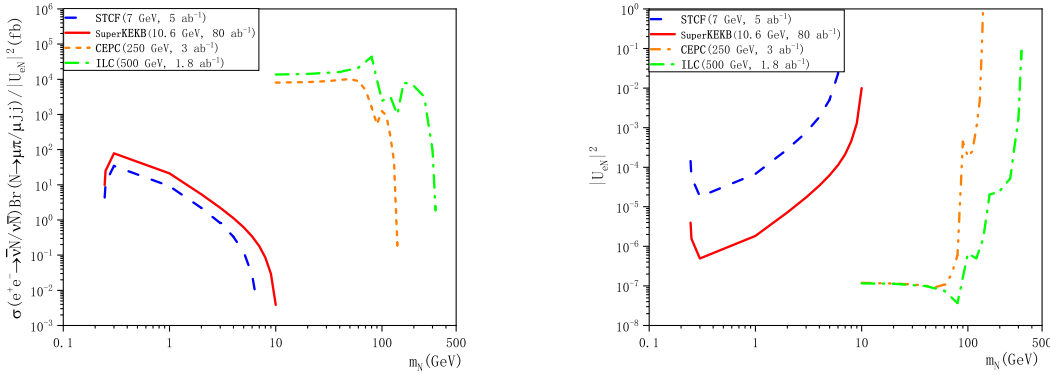


FIG. 2: The cross section of sterile neutrino N production in Drell-Yan(Z) and W -exchange channels at the e^+e^- collider and the $|U_{eN}|^2$ sensitivity at the 95% confidence level. Here for light N , $N \rightarrow \mu\pi$ is used; while for heavy N , $N \rightarrow \mu jj$ is adopted. The inflections are caused by signal cuts and definition of Γ_N .

At the STCF and the SuperKEKB, we construct the signal via $N \rightarrow \mu\pi$ and missing energy, the main background comes from $e^+e^- \rightarrow W^*W^* \rightarrow \mu\bar{\nu}_\mu\pi$ which is negligible small due to double weak coupling at low center-of-mass energy, hence we neglect the background in our analysis. At the CEPC and the ILC, the signal is composed of μjj with missing energy, and there tend to be small open angle between the signal lepton and jets for more energetic N , while the open angle is relative large in the background $e^+e^- \rightarrow W^*W^* \rightarrow \mu\bar{\nu}_\mu jj$ due to lepton and jets origin from different W boson. Hence we impose the open angle cut for signal selection at the CEPC (ILC): $\sum \theta_{\ell jj} < 160^\circ$ is adopted for $m_N < 80$ (150) GeV, the background can be ruled out with cut; while $\sum \theta_{\ell jj} <$

270° (240°) for $m_N > 80$ (150) GeV with the background is cut to be 0.0557(0.0167) pb. The basic cuts are used for the analysis at the CEPC and the ILC: $p_T^{\ell,j} > 10$ GeV, $|\eta^{\ell,j}| < 5$ and $\cancel{E}_T > 10$ GeV.

According to our numerical results, see FIG.2, the cross sections are sub-fb to tens of pb with the increase of \sqrt{s} from the STCF to the ILC. Considering that the integrated luminosity of those facilities is large, the signatures for GeV sterile neutrino can be well explored and hence make a constrain for active-sterile mixing $|U_{\ell N}|^2$. The constrain can be estimated by solving $\frac{N_s}{\sqrt{N_s+N_B}} \approx 1.7$ which means signal significance at the 95% confidence level [33], where $N_{s/B}$ is the signal/background events number. At the STCF, the center-of-mass energy can reach 7 GeV, the lower-limit of $|U_{eN}|^2$ can reach $10^{-3} - 10^{-4}$ at 0.3-2 GeV with 5 ab^{-1} integrated luminosity. While for the SuperKEKB, the constrains can be further extended due to high luminosity. At the high energy electron-positron collider, the CEPC and ILC, the physics potential for sterile neutrino searches can be extended to hundreds GeV level with $|U_{eN}|^2$ sensitivities of $10^{-3} - 10^{-6}$.

B. ep collision

In this section, we explore the production mechanism of sterile neutrino in the context of γ - W^* interaction at the future ep colliders, where the photon is produced via proton bremsstrahlung [34], the distribution function of photon is given in FIG.3. The photon from proton bremsstrahlung tends to less energetic compared with electron bremsstrahlung and laser back scattering, while the collider signature is relative clear due to the unbroken proton, generally several light jets are generated via broken proton and the signal jets could get submerged in complex jets background.

The energy spectrum of proton bremsstrahlung photon can be well formulated in Weizsacker-Williams approximation (WWA-p) [34]

$$f_\gamma^p(x) = \frac{\alpha}{2\pi} \frac{2}{x} \left\{ \left[1 - x + \frac{x^2}{4}(1 + 4a + \mu_p^2) \right] I + (\mu_p^2 - 1) \left[1 - x + \frac{x^2}{4} \right] I' - \frac{1-x}{z^3} \right\}, \quad (5)$$

where $\mu_p = 2.79$, $a = 4.96$, $z = 1 + \frac{a}{4} \frac{x^2}{1-x}$ and

$$I = -\ln\left(1 - \frac{1}{z}\right) - \frac{1}{z} - \frac{1}{2z^2} - \frac{1}{3z^3} \quad (6)$$

$$I' = -\frac{1}{(a-1)^4} \ln\left(1 + \frac{a-1}{z}\right) + \frac{1}{(a-1)^3 z} - \frac{1}{2(a-1)^2 z^2} + \frac{1}{3(a-1)z^3}. \quad (7)$$

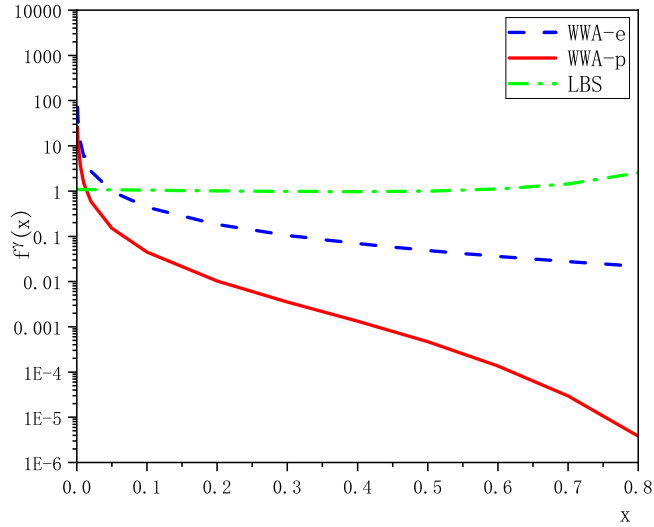


FIG. 3: The distribution function of photon through electron/proton bremsstrahlung (WWA-e/p) and laser back scattering (LBS).

The total cross section can be expressed as the convolution of the $e^- + \gamma \rightarrow N + W^-$ cross section with the photon distribution function,

$$\sigma = \int dx f_\gamma^p(x) \hat{\sigma}(e^- \gamma \rightarrow NW^-) \quad (8)$$

$$\hat{\sigma}(e^- \gamma \rightarrow NW^-) = \frac{1}{2} \frac{1}{2} \frac{1}{2s} \frac{1}{8\pi s} \int_{t^-}^{t^+} |\mathcal{M}(e^- \gamma \rightarrow NW^-)|^2 dt, \quad (9)$$

where the Mandelstam variables are define as $s = (p_{e^-} - p_\gamma)^2$, $t = (p_{e^-} - p_N)^2$, $t^\pm = \frac{m_N^2 + m_W^2 - s \pm \sqrt{\lambda(s, m_N^2, m_W^2)}}{2}$ with the Källén function $\lambda(x, y, z) \equiv (x - y - z)^2 - 4yz$; the first two $\frac{1}{2}$ are spin-polarization average factors of electron and photon; $\frac{1}{2s}$ and $\frac{1}{8\pi s}$ are the flux and two-body final state phase space factor.

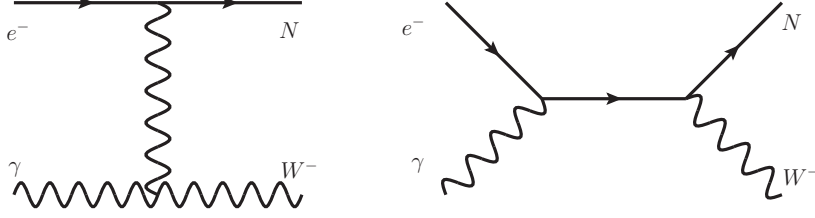


FIG. 4: The Feynman diagrams for heavy sterile neutrino production through $e^- \gamma \rightarrow NW^-$ channel, where the photon is produced via proton bremsstrahlung.

The amplitude square for $e^- \gamma \rightarrow NW^-$ is

$$\begin{aligned}
|\mathcal{M}|^2 = & -\frac{|U_{eN}|^2}{2m_W^2 s(m_W^2 - t)^2 s_w^2} \{2m_N^6(m_W^2 - t) + m_N^4[6m_W^4 - 8m_W^2 t + t(s + 2t)] \\
& + m_N^2[-6m_W^6 - 2m_W^4(3s + 2t) + m_W^2(9s^2 + 14st + 12t^2) + t(s^2 - st - 2t^2)] \\
& + 4m_W^2[m_W^6 - m_W^4(3s + t) + m_W^2(2s + t)^2 - 2s^3 - 4s^2 t - 3st^2 - t^3]\}. \quad (10)
\end{aligned}$$

In this section, we consider the production of sterile neutrino through $e^- \gamma \rightarrow NW^-$ channel at the future electron-proton collider, *i.e.*, the LHeC. For the events reconstruction, $N \rightarrow \mu jj$ channel is adopted, while the W boson is reconstructed via hadronic channel with $Br(W^- \rightarrow jj) \approx 65\%$. The LHeC is designed to reach a luminosity of 1.05×10^{34} , led to approximately 1 ab^{-1} integrated luminosity for 10 years operation. Furthermore, the Dirac or Majorana nature of the sterile neutrino can be identified via the sign of single lepton, *e.g.*, $N \rightarrow \ell^+ jj$ only for Majorana neutrino, while $N \rightarrow \ell^- jj$ for both Dirac and Majorana neutrino.

The incoming electron/proton beam energy at the LHeC is 60/7000 GeV, leads to the center of mass energy $\sqrt{s} = 1296 \text{ GeV}$. The WWA-p photon will be produced at the LHeC through high energy proton bremsstrahlung, therefore it provides a better condition for researching new phenomena due to clear background. The signal for $e^- \gamma \rightarrow NW^-$ channel is $\mu^- + \text{di-jet} + \text{W-jet}$ without missing energy, the di-jet may appears to be fat jet origins from N decay and the W-jet is generally composed of two prong jets. The main background signals come from $e^- + \gamma \rightarrow \nu_e + Z + W^-$ where Z decays into $\ell \bar{\nu}_\ell + jj$, and $e^- + \gamma \rightarrow \nu_e + W^- + W^- + W^+$ with W decays into leptons or jets, the two cross sections are below experiments tag limit $1/\int \mathcal{L} \approx 1 \text{ ab}$. In the next analysis,

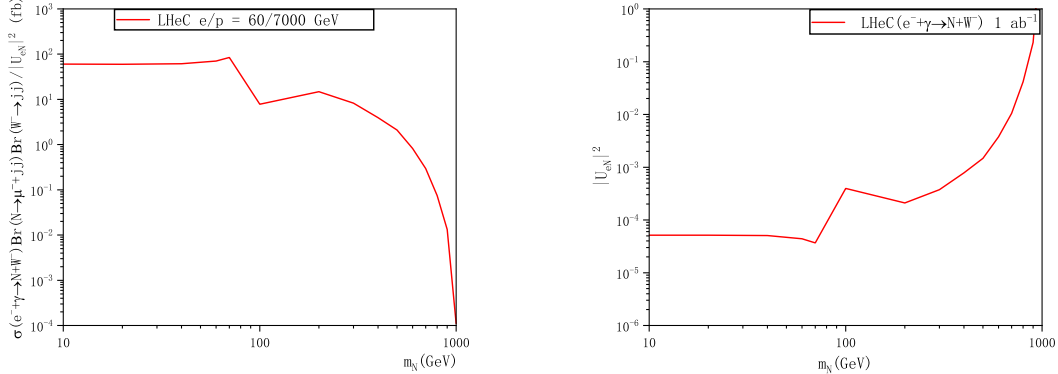


FIG. 5: *Left*: The canonical production cross section of $e^- \gamma \rightarrow NW^-$ at the LHeC with basic cuts. Here the photon is produced through proton bremsstrahlung. *Right*: The sensitivities of sterile and active neutrino mixing $|U_{eN}|^2$ at the 95% confidence level with integrated luminosity of 1 ab^{-1} at the LHeC. Here $Br(N \rightarrow \mu^- jj)$ and $Br(W^- \rightarrow jj)$ are taken into account for N and W boson reconstruction. The inflection near m_W is caused by the definition of sterile neutrino total width.

we adopt the basic cuts (BC) for lepton and jets: $p_T^{\ell,j} > 10 \text{ GeV}$, $|\eta^{\ell,j}| < 5$.

In the FIG.5, the cross sections for $e^- \gamma \rightarrow NW^-$ and $|U_{eN}|^2$ sensitivity at the LHeC are given. According to our analysis, the canonical production cross section for $e^- \gamma \rightarrow NW^-$ process will reach hundreds of fb for the electroweak energy mass scale sterile neutrino. The cross section decreases to tens of fb when for $m_N \sim 500 \text{ GeV}$, and hence provides tests for heavy sterile neutrino in this region which is poorly constrained. The sensitivity of active-sterile neutrino mixing $|U_{eN}|^2$ with $100 < m_N < 500 \text{ GeV}$ is estimated to be $10^{-3} \sim 10^{-4}$ level, therefore provide helpful information to search the heavy sterile neutrino in this region.

III. INDIRECT PRODUCTION

A. Kink search via B meson semileptonic decay

The sterile neutrino can be also investigated by searching kinks in lepton energy spectrum of the B meson semileptonic decay, see earlier nucleus β -decay spectrum kink search [35]. The mechanism is straightforward, in three-body decay $B \rightarrow D + \ell\nu$, the maximal lepton energy in B meson rest frame is $E_\ell = \frac{m_B^2 + m_\ell^2 - (m_D + m_\nu)^2}{2m_B}$. If the sterile neutrino mass is in GeV, which led to kink at giving energy point in the spectrum, see FIG.6 for diagrammatic sketch. The previous research focus on Nucleus or π, K beam-dump experiments, in which π, K are stopped, *e.g.*, by plastic scintillator inside a homogeneous magnetic field [36]. While at the SuperKEKB B-factory, B meson is produced nearly rest, thus can be applied for kink search.

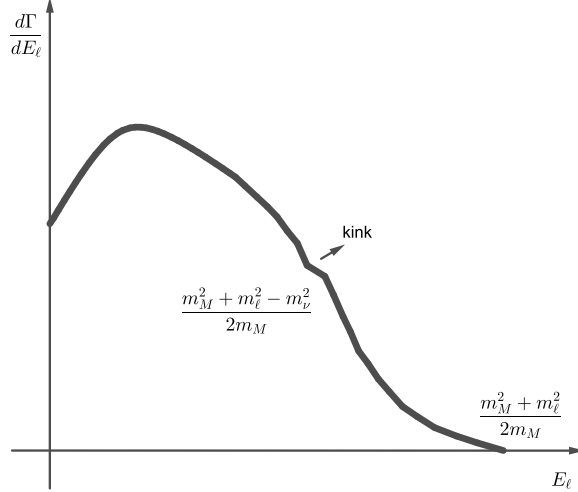


FIG. 6: Schematic kink structure in lepton energy spectrum of β -decay.

The SuperKEKB, with design luminosity of $8 \times 10^{35} \text{ cm}^{-2}\text{s}^{-1}$, will produce $2.7 \times 10^{10} \Upsilon(4S)$ [$\sigma(e^+e^- \rightarrow \Upsilon(4S)) = 1.08 \text{ nb}$] at Υ resonant energy [37] per-year. The $B\bar{B}$ (approximately stopped) number can be estimated by half the $\Upsilon(4S)$ yields, hence

there will be 1.35×10^{10} $B\bar{B}$ -pair. Suppose as an estimation that

$$Br(B \rightarrow D + \ell N) \sim |U_{\ell N}|^2 Br(B \rightarrow D + \ell \nu) = 2.2 \times 10^{-2} |U_{\ell N}|^2, \quad (11)$$

and the D meson can be reconstructed via $K + n\pi$ -channel,

$$Br(D^+ \rightarrow K^- + 2\pi^+) = 9.38\%, Br(\bar{D}^0 \rightarrow K^- + \pi^+) = 3.94\%.$$

Therefore the low sensitivity limit for $|U_{\ell N}|^2$ can be extended to 10^{-7} -level at $1 - 4$ GeV mass region. What deserves mentioning here is the decay length of N may be far long than detector size ($L \sim 1$ m), hence the directly reconstructed signal of N will suppressed by factor $1 - \exp[-\frac{L}{c\tau_N\gamma\beta}]$, typically $10^{-4} \sim 10^{-2}$ in this mass region, so the direct search of N may be limited, therefore the kink method will provide another insight in sterile neutrino searching. The same techniques can be used in the BES-III via $\Psi(3770) \rightarrow D\bar{D}$.

B. Meson Decay

The $0\nu\beta\beta$ decay branching ratios of charged meson ($\pi, K, D_{(s)}, B_{(s,c)}$) induced by W^*W^* is too small, encounters a severe suppression either due to the small neutrino mass like $\frac{m_N^2}{m_W^2}$ or due to the small mixing $|U_{\ell N}U_{\ell' N}|^2$, lack of experiment interest at present. Typically, the $K^+ \rightarrow \pi^- + \mu^+\mu^+$ branching ratio for heavy sterile neutrino is [38]:

$$Br(K^+ \rightarrow \pi^- + \mu^+\mu^+) \sim 1.6 \times 10^{-12} \left(\frac{1 \text{ GeV}}{m_N}\right)^2 |U_{\mu N}|^4$$

However, if the neutrino mass lie between $m_\pi + m_\mu \leq m_N \leq m_K - m_\mu$, the branching ratio can be greatly enhanced by resonant effect [39]. In the narrow resonance approximation, the decay rate can be formulated as

$$\Gamma(M_1 \rightarrow M_2 + \ell\ell) = \Gamma(M_1 \rightarrow \ell N) \frac{\Gamma(N \rightarrow \ell + M_2)}{\Gamma(N)} \quad (12)$$

Hence, the branching ratio can be easily estimated by leptonic ratio of meson times $N \rightarrow \ell + M$ decay ratio, which is approximately several persents. The number of

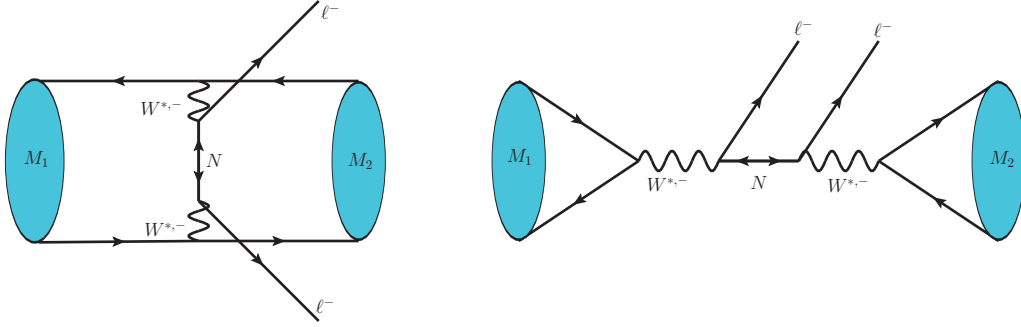


FIG. 7: $0\nu\beta\beta$ decay and sterile neutrino resonant decay of meson.

TABLE II: The leptonic decay fraction of K, D, D_s, B, B_c , the $e^+\nu_e$ branching ratio are tiny due to small electron mass.

Br	K^+ [40]	D^+ [40]	D_s^+ [40]	B^+ [41]	B_c^+ [42]
$\mu^+\nu_\mu$	0.635	3.74×10^{-4}	5.43×10^{-3}	4.3×10^{-7}	6.2×10^{-5}
$\tau^+\nu_\tau$	-	1.2×10^{-3}	5.3×10^{-2}	1.09×10^{-4}	1.47×10^{-2}

D/B meson produced at LHC is estimated to be about $10^{13}/10^{12}$, there are extensive investigation upon this topic, thus provide experimental limits on sterile neutrino mixing elements ($|U_{\ell N}|$) in mass region of $m_N = 1 \sim 4$ GeV.

C. Baryon decay

The resonant mechanism can be easily extended in baryon semileptonic decay, *i.e.*, $B_1 \rightarrow B_2 + \ell N (\rightarrow \ell\pi)$, the branching ratio can be factorized as,

$$Br(B_1 \rightarrow B_2 + \ell\ell + \pi) = \frac{\Gamma(B_1 \rightarrow B_2 + \ell N)}{\Gamma(B_1)} \frac{\Gamma(N \rightarrow \ell\pi)}{\Gamma(N)}, \quad (13)$$

where $\Gamma_{B_1/N}$ is the total decay width of initial meson (N).

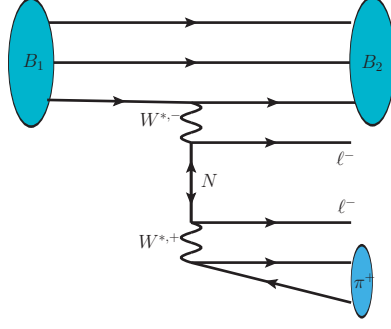


FIG. 8: $0\nu\beta\beta$ decay of baryon.

The secondary decay width is well known,

$$\Gamma(N \rightarrow \ell\pi) = \frac{G_F^2}{16\pi} |V_{ud}|^2 |U_{\ell N}|^2 f_\pi^2 m_N \sqrt{\lambda(m_N^2, m_\ell^2, m_\pi^2)} \left[\left(1 - \frac{m_\ell^2}{m_N^2}\right)^2 - \frac{m_\pi^2}{m_N^2} \left(1 + \frac{m_\ell^2}{m_N^2}\right) \right], \quad (14)$$

where we set $m_\pi = 139$ MeV, $f_\pi = 130.4$ MeV, $m_\mu = 105$ MeV for numerical analysis.

The Feynman diagram for this process is shown in FIG.8, the amplitude can be formulated as

$$\mathcal{M}(B_1 \rightarrow B_2 + \ell N) = \frac{G_F}{\sqrt{2}} V_{q_1 q_2} U_{\ell N} \langle B_2 | \bar{q}_2 \gamma^\mu (1 - \gamma^5) q_1 | B_1 \rangle [\bar{\ell} \gamma_\mu (1 - \gamma^5) N], \quad (15)$$

where the CKM matrix elements are taken as: $V_{ud} = 0.9737$, $V_{cs} = 0.975$, $V_{cd} = 0.221$, $V_{cb} = 4.08 \times 10^{-2}$.

The hadronic transition matrix elements for the semileptonic decay can be parameterized in terms of six invariant form factors,

$$\begin{aligned} \langle B_2 | \bar{q}_2 \gamma^\mu (1 - \gamma^5) q_1 | B_1 \rangle &= \bar{u}(B_2) [\gamma^\mu f_1(q^2) + i\sigma^{\mu\nu} q_\nu \frac{f_2(q^2)}{m_{B_1}} + q^\mu \frac{f_3(q^2)}{m_{B_1}}] u(B_1) \\ &\quad - \bar{u}(B_2) [\gamma^\mu g_1(q^2) + i\sigma^{\mu\nu} q_\nu \frac{g_2(q^2)}{m_{B_1}} + q^\mu \frac{g_3(q^2)}{m_{B_1}}] \gamma^5 u(B_1), \end{aligned} \quad (16)$$

where $u(B_{1/2})$ are Dirac spinors of the initial/final baryon with $q = p_{B_1} - p_{B_2}$.

Note that a considerable number of heavy baryon can be produced at the LHC, hence provides opportunity for experiment search of the sterile neutrino induced four-body decay. In the previous research [31, 43], $\Lambda_{b/c}$ baryon has been considered. In this

section, we explore the four-body $|\Delta L| = 2$ decays of the $\Xi_{cc}^{++}, \Xi_c^+, \Xi_c^0$ baryon,

$$\begin{aligned}\Xi_{cc}^{++} &\rightarrow \Xi_c^+ + \mu^+ \mu^+ \pi^-, \\ \Xi_{cc}^{++} &\rightarrow \Lambda_c^+ + \mu^+ \mu^+ \pi^-, \\ \Xi_c^+ &\rightarrow \Xi^0 + \mu^+ \mu^+ \pi^-, \\ \Xi_c^0 &\rightarrow \Xi^- + \mu^+ \mu^+ \pi^-, \end{aligned}$$

which can occur via the exchange of Majorana neutrino with kinematically allowed mass, $m_\mu + m_\pi < m_N < m_{B_1} - m_{B_2} - m_\mu$. Within this mass region, the narrow width approximation [32] is valid due to $\Gamma_N \ll m_N$. For numerical evaluation, we use the form factor for $\Xi_{cc}^{++} \rightarrow \Xi_c^+$ [44], $\Xi_{cc}^{++} \rightarrow \Lambda_c$ [45], $\Xi_c^+ \rightarrow \Xi^0$ [46], $\Xi_c^0 \rightarrow \Xi^-$ [46] among those references respectively, the canonical branching fraction $\frac{Br(B_1 \rightarrow B_2 + \mu\mu\pi)}{|U_{\mu N}|^2}$ is given in FIG. 9.

At the LHC, the production number of heavy baryon can be estimated by fragmentation fraction of c-quark and b-quark, $f(c \rightarrow \Lambda_c^+) = 20.4\%$ [47], $f(c \rightarrow \Xi_c^0) = 8\%$ [47], $f(b \rightarrow \lambda_b^0) = 25.9\%$ [48], and the production cross section for $c\bar{c}$ and $b\bar{b}$ are measured to be $2369 \mu\text{b}$ [49] and $144 \mu\text{b}$ [50] at the LHCb with $\sqrt{s} = 13 \text{ TeV}$. Suppose the LHCb accumulate an integrated luminosity of approximately 50 fb^{-1} at the end of LHC Run-4 till 2035, hence we will get $N(\Lambda_c) = 2 \times 50 \text{ fb}^{-1} \times 2369 \mu\text{b} \times 20.4\% = 4.83 \times 10^{13}$, $N(\Xi_c^0) = 2 \times 50 \text{ fb}^{-1} \times 2369 \mu\text{b} \times 8\% = 1.90 \times 10^{13}$, $N(\Lambda_b) = 2 \times 50 \text{ fb}^{-1} \times 144 \mu\text{b} \times 25.9\% = 3.73 \times 10^{12}$. The production cross section of Ξ_c^+ [51] is measured to be $14.9 \mu\text{b}$, the production number is estimated to be $N(\Xi_c^+) = 2 \times 50 \text{ fb}^{-1} \times 14.9 \mu\text{b} = 1.49 \times 10^{12}$. The production cross section of Ξ_{cc}^{++} can be estimated via its decay fraction versus Λ_c^+ [52], $\frac{\sigma(\Xi_{cc}^{++}) Br(\Xi_{cc}^{++} \rightarrow \Lambda_c^+ K^- \pi^+ \pi^+)}{\sigma(\Lambda_c^+)} = 2.22 \times 10^{-4}$, and the fraction for $Br(\Xi_{cc}^{++} \rightarrow \Lambda_c^+ K^- \pi^+ \pi^+)$ is approximately 1.5% [53], hence the fraction $\frac{\sigma(\Xi_{cc}^{++})}{\sigma(\Lambda_c^+)} = 1.48\%$, led to $N(\Xi_{cc}^{++}) = 4.83 \times 10^{13} \times 1.48\% = 7.15 \times 10^{11}$. The production number of above heavy baryon is organized into TABLE.III.

Experimental limits from the search of above $|\Delta L| = 2$ processes can be reinterpreted as constrains on the sterile neutrino mixing matrix elements $|U_{\mu N}|^2$ versus m_N , hence one need to estimate the detection efficiency. Precise computation of the detection efficiency requires fully simulated decay-specific Monte Carlo samples, that is reconstructed

TABLE III: The estimated production number of heavy baryon at the LHCb in 13 TeV at an accumulated luminosity of 50 fb^{-1} .

	Λ_c^+	Λ_b^0	Ξ_{cc}^{++}	Ξ_c^+	Ξ_c^0
number(10^{12})	48.3	3.73	0.715	1.49	19.0

TABLE IV: The mass and lifetime of heavy baryon.

	Λ_c^+	Λ_b^0	Ξ_{cc}^{++}	Ξ_c^+	Ξ_c^0
mass(GeV)	2.286	5.619	3.621	2.467	2.470
lifetime(fs)	201	1464	256	453	151

in the same manner as real data and with a simulation of the full detector, which is out of the range of this paper. Based on the above analysis, here we explore the constrains of $|U_{\mu N}|^2$ from the experimental searches on $\Lambda_c^+ \rightarrow \Lambda \mu^+ \mu^+ \pi^-$, $\Lambda_b^0 \rightarrow \Lambda_c^+ \mu^- \mu^- \pi^+$, $\Xi_{cc}^{++} \rightarrow \Xi_c^+ \mu^+ \mu^+ \pi^-$, $\Xi_{cc}^{++} \rightarrow \Lambda_c^+ \mu^+ \mu^+ \pi^-$, $\Xi_c^+ \rightarrow \Xi^0 \mu^+ \mu^+ \pi^-$, $\Xi_c^0 \rightarrow \Xi^- \mu^+ \mu^+ \pi^-$ at the LHCb with the 95% confidence level, that is $N(B_1)Br(B_1 \rightarrow B_2 + \mu\mu\pi)Br(B_2 \rightarrow X)\epsilon_{eff} = 3.09$. Considering the values found for the cross section and efficiencies at the 95% confidence level, FIG.9 shows the constrains for $|U_{\mu N}|^2$ versus m_N at the LHCb in 13 TeV with an integrated luminosity of 50 fb^{-1} . The final state baryon Λ , Ξ^0 , Ξ^- , Λ_c^+ , Ξ_c^+ are reconstructed via $\Lambda \rightarrow p\pi^-$, $\Xi^0 \rightarrow \Lambda(\rightarrow p\pi^-)\pi^+$, $\Xi^- \rightarrow \Lambda(\rightarrow p\pi^-)\pi^-$, $\Lambda_c \rightarrow pK^-\pi^+$, $\Xi_c^+ \rightarrow pK^-\pi^+$ channels respectively, the branching fraction are listed in TABLE V.

According to the above analysis, the $|U_{\mu N}|^2 - m_N$ planes are give in FIG.9. As the branching fraction for heavy baryon four-body decay reach its maximal value just above $\mu\pi$ threshold $\gtrsim 252\text{MeV}$, the constrain for $|U_{\mu N}|^2$ is strongest here. For $\Lambda_c \rightarrow \Lambda \mu^+ \mu^+ \pi^-$ channel, the maximal branching fraction can reach several part-per-thousand, and the Λ_c can be numerous produced at LHCb, the lower-limit for $|U_{\mu N}|^2$ can reach $\times 10^{-8}$ at $0.25 < m_N < 0.5 \text{ GeV}$. The fraction of charm quark fragment into Ξ_c is smaller

TABLE V: The reconstruction channels and detection efficiencies of heavy baryon $\Lambda_c, \Lambda_b, \Xi_{cc}^{++}, \Xi_c^+, \Xi_c^0$ four-body decay. The branching fraction of secondary decay chain is adopted from [40]. The detection efficiency for $\Lambda_{b/c}$ is adopted according to estimation of previous research [31, 43], the efficiency for Ξ_c^+, Ξ_c^0 is estimated from similar decay channels at LHCb [54]. Due to the experimental investigation of new discovered double-charmed Ξ_{cc}^{++} is poor, hence we approximately set the detection efficiency to be 1×10^{-4} .

	$\Lambda_c^+ \rightarrow \Lambda \mu^+ \mu^+ \pi^-$	$\Lambda_b^0 \rightarrow \Lambda_c^+ \mu^- \mu^- \pi^+$	$\Xi_{cc}^{++} \rightarrow \Xi_c^+ \mu^+ \mu^+ \pi^-$	$\Xi_{cc}^{++} \rightarrow \Lambda_c^+ \mu^+ \mu^+ \pi^-$	$\Xi_c^+ \rightarrow \Xi^0 \mu^+ \mu^+ \pi^-$	$\Xi_c^0 \rightarrow \Xi^- \mu^+ \mu^+ \pi^-$
channel	$\Lambda \rightarrow p \pi^-$ 64.1%	$\Lambda_c^+ \rightarrow p K^- \pi^+$ 6.26%	$\Xi_c^+ \rightarrow p K^- \pi^+$ 0.62%	$\Lambda_c^+ \rightarrow p K^- \pi^+$ 6.26%	$\Xi^0 \rightarrow p \pi^- \pi^+$ 63.8%	$\Xi^- \rightarrow p \pi^- \pi^-$ 64.0%
efficiency	1×10^{-3} [31]	9.8×10^{-3} [43]	1×10^{-4}	1×10^{-4}	1.18×10^{-2} [54]	1.1×10^{-3} [54]

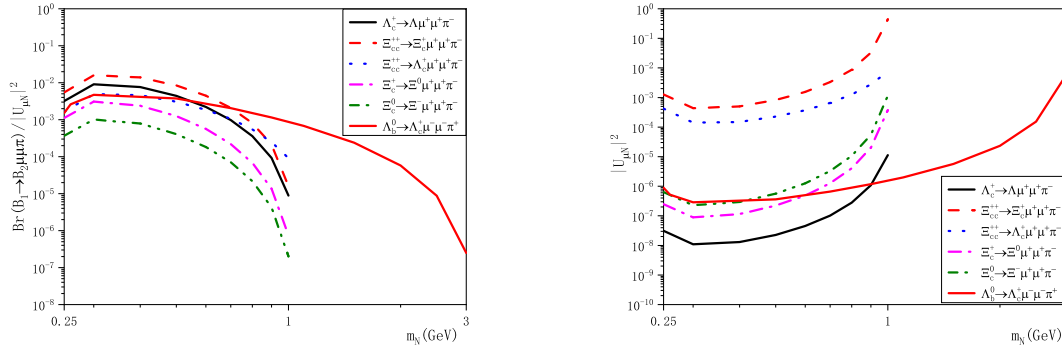


FIG. 9: The canonical branching fraction of sterile neutrino exchange four-body heavy baryon decay, and the sensitivity of $|U_{\mu N}|^2$ at the LHCb with an integrated luminosity of 50 fb^{-1} at the 95% confidence level.

compare with Λ_c^+ , and the branching fractions for $\Xi_c^+ \rightarrow \Xi^0 \mu^+ \mu^+ \pi^-$, $\Xi_c^0 \rightarrow \Xi^- \mu^+ \mu^+ \pi^-$ are in part-per-thousand, hence the lower-limits for $|U_{\mu N}|^2$ are shifted by one magnitude around 10^{-7} at the same m_N mass region. We also explore the decay channels for double-charmed baryon Ξ_{cc}^{++} via $\Xi_{cc}^{++} \rightarrow \Xi_c^+ \mu^+ \mu^+ \pi^-$, $\Xi_{cc}^{++} \rightarrow \Lambda_c^+ \mu^+ \mu^+ \pi^-$, although the branching fractions are not small, the constrains are weak for less produced number and inefficiency. As pointed in previous research [31, 43], the bottom baryon Λ_b^0 can also

provide unique test with broad mass region $0.3 \sim 3.0$ GeV.

D. Higgs Decay

The collider search for massive sterile neutrino via Higgs boson decay channels also provide a interesting test, especially for heavier mass as the Yukawa coupling is proportional to fermion mass. In reference [55, 56], the author explore direct coupling of Higgs $\rightarrow \nu N$. In contrast, if the sterile neutrino mass lie much below Higgs mass, the coupling strength will dramatically suppressed, in this case the Higgs $\rightarrow WW(\rightarrow \mu\mu\pi)$ decay channel may be also provide an unique test. Furthermore, at least one missing energy is required for the construction of direct decay channel, while final state products of the Higgs $\rightarrow WW(\rightarrow \mu\mu\pi)$ channel can be fully reconstructed and the $|\Delta L| = 2$ same-sign $\mu\mu$ event is an obvious new physics signal.

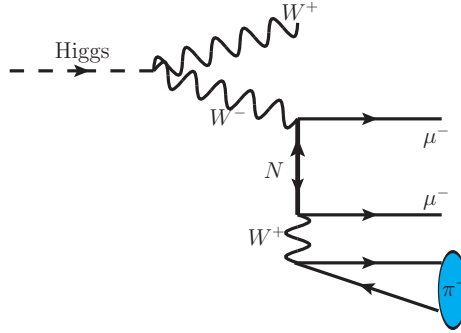


FIG. 10: Sterile neutrino production via Higgs $\rightarrow WW(\rightarrow \mu\mu\pi)$ channel.

In this section, we calculate the branching fraction for Higgs $\rightarrow WW(\rightarrow \mu\mu\pi)$, the decay width can be formulated as

$$\Gamma(\text{H} \rightarrow W^+ \mu^- \mu^- \pi^+) = \Gamma(\text{H} \rightarrow W^+ \mu^- N) \frac{\Gamma(N \rightarrow \mu^- \pi^+)}{\Gamma(N)}, \quad (17)$$

where narrow resonance approximation for sterile neutrino N is adopted.

According to (1), the decay amplitude is written as

$$\mathcal{M}(\text{H} \rightarrow W^+ \mu^- N) = -\frac{4m_W^3 G_F U_{\mu N}}{(p_N + p_\pi)^2 - m_W^2} \epsilon_\mu^*(p_W) \bar{u}(p_\mu) \gamma^\mu \gamma_L u(p_N), \quad (18)$$

where $\epsilon_\mu^*(p_W)$ is the polarization vector of final W^+ boson, $\gamma_L = \frac{1 - \gamma^5}{2}$. The amplitude square is

$$|\mathcal{M}(H \rightarrow W^+ \mu^- N)|^2 = \frac{16G_F^2 m_W^4 |U_{\mu N}|^2}{(m_H^2 + m_\mu^2 + m_N^2 - s_1 - s_3)^2} [m_H^2 m_W^2 + m_\mu^2 (m_N^2 + m_W^2 - s_3) + (m_N^2 + 2m_W^2)(m_W^2 - s_1) + s_3(s_1 - 2m_W^2)], \quad (19)$$

where we define $s_1 = (p_W + p_\mu)^2$, $s_2 = (p_W + p_N)^2$.

The decay width can be formulated as

$$\Gamma(H \rightarrow W^+ \mu^- N) = \frac{1}{2m_H} \frac{1}{(2\pi)^5} \frac{\pi^2}{4m_H^2} \int_{(m_\mu + m_W)^2}^{(m_H - m_N)^2} ds_1 \int_{s_2^-}^{s_2^+} ds_2 |\mathcal{M}(H \rightarrow W^+ \mu^- N)|^2 \quad (20)$$

Here $s_2^\pm = m_W^2 + m_N^2 - \frac{(s_1 - m_H^2 + m_N^2)(s_1 + m_W^2 - m_\mu^2) \mp \lambda^{1/2}(m_H^2, s_1, m_N^2) \lambda^{1/2}(s_1, m_W^2, m_\mu^2)}{2s_1}$, and $\frac{1}{(2\pi)^5} \frac{\pi^2}{4m_H^2}$ is the factor for three-body final state phase space. We set $m_H = 125$ GeV, $\Gamma_H = 3.2$ MeV in the calculation.

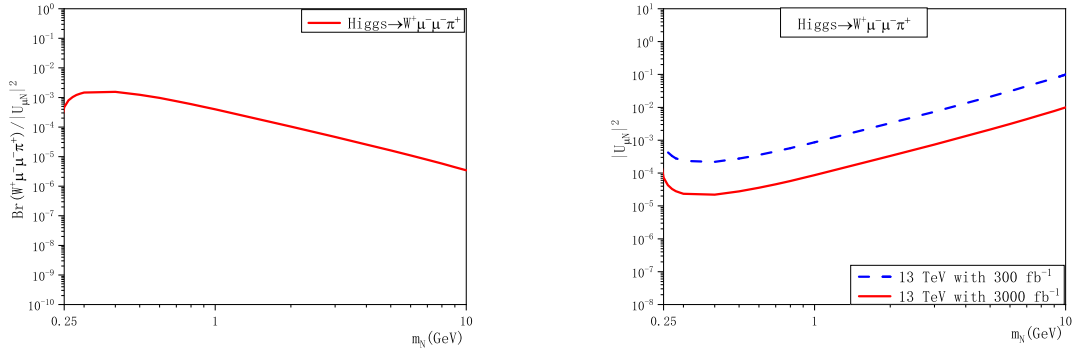


FIG. 11: Branching fraction for Higgs $\rightarrow WW(\rightarrow \mu\mu\pi)$ and the $|U_{\mu N}|^2$ sensitivity at the 95% confidence level in 13 TeV LHC with integrate luminosity of 300/3000 fb^{-1} respectively. Here the production cross section of Higgs is estimated to be 50 pb, and the W boson is reconstructed via $c\bar{s}$ -jet channel. The charge conjugate is hold here.

At the LHC, Higgs boson is mainly produced via gluon-gluon-fusion channel with cross section of $\sigma_{ggF}(pp \rightarrow \text{Higgs} + X) \sim 50$ pb. The ATLAS has accumulated an integrated luminosity $\sim 150 \text{ fb}^{-1}$, means 7.5×10^6 Higgs. After LHC update, the integrated

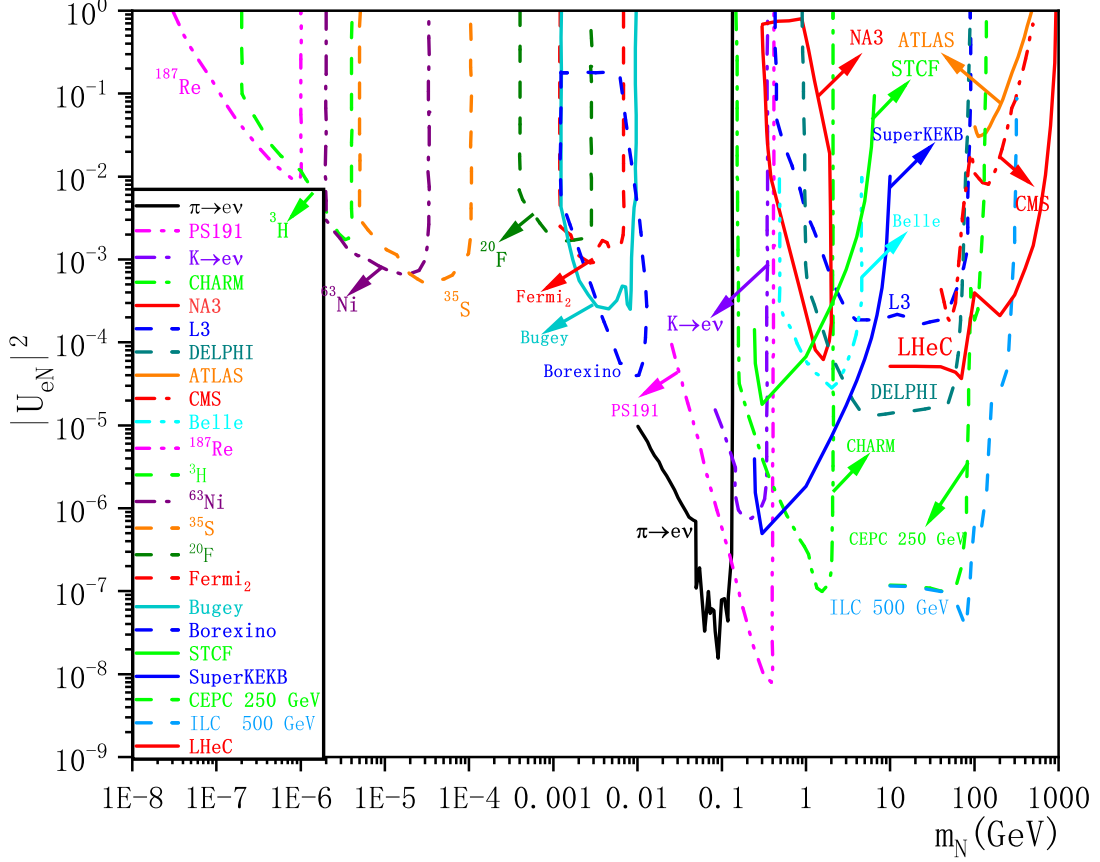


FIG. 12: Bounds on active-sterile mixing $|U_{eN}|^2$ from various experiments and this article. Kink search: ^{187}Re [7], ^3H [8], ^{63}Ni [9], ^{35}S [10], ^{20}F [11], Fermi₂ [11]; N decay search: Borexino [57], Bugey [58], CMS [27]; Peak search: $\pi \rightarrow e\nu$ [12], $K \rightarrow e\nu$ [13]; Beam-dump: PS191 [59], NA3 [60], CHARM [61]; Z^0 decay: DELPHI [21], L3 [20]; B meson decay: Belle [62]; Direct production search: ATLAS [25]

luminosity will be in 3000 fb^{-1} level, hence the produced Higgs can reach 1.5×10^8 . Such abundant Higgs events will put new sight in sterile neutrino search. Compared with direct Higgs $\rightarrow \nu N$ decay, the Higgs $\rightarrow WW(\rightarrow \mu\mu\pi)$ channel can be easily detected and the new physics signal is much more clear. We analyze the branching fraction

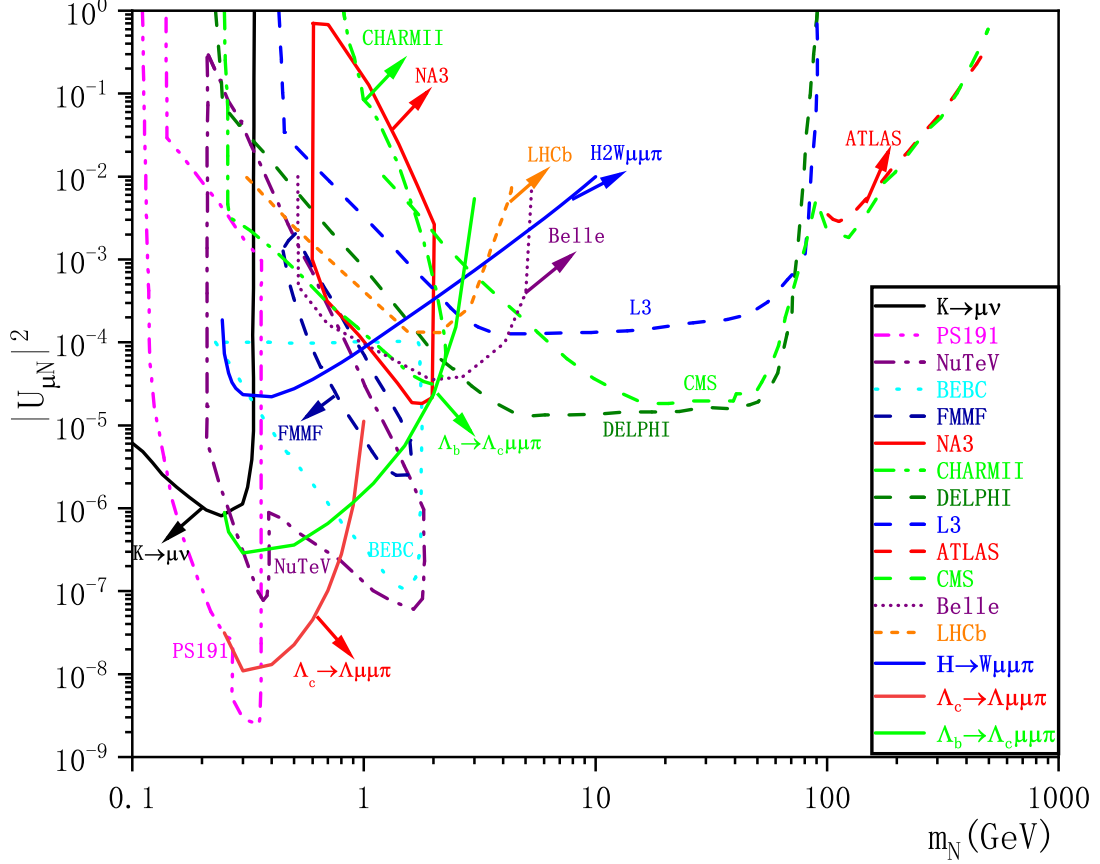


FIG. 13: Current bounds on active-sterile mixing $|U_{\mu N}|^2$ from various experiments and this article. Peak search: $K \rightarrow \mu\nu$ [63]; Beam-dump: PS191 [59], NA3 [60], CHARMII [64], BEBC [65]; Z^0 decay: DELPHI [21], L3 [20], FMMF [66], NuTeV [67]; B meson decay: Belle [62], LHCb [18]; N decay search: CMS [27]; Direct production search: ATLAS [25].

of this channel, see FIG.11, with m_N lie between $m_\mu + m_\pi$ and $m_H - m_W - m_\mu$. The fraction reaches maximal value at m_N mass slightly above $m_\mu + m_\pi$ threshold, and decreases dramatically in high mass region. We analyze the constrain for $|U_{\mu N}|^2$ at the 95% confidence level, suppose that W boson is reconstructed via $c\bar{s}$ -jet channel with $Br(W^+ \rightarrow c\bar{s}) = 30\%$. The $|U_{\mu N}|^2 - m_N$ plane is given in FIG.11. The lower-limit of

$|U_{\mu N}|^2$, reach 10^{-5} , lies just above $m_\mu + m_\pi$ threshold. Hence we recommend an experimental investigation in this mass region, the signal is obvious and the background is relatively clear.

IV. SUMMARY AND CONCLUSIONS

In summary, we have studied the production mechanisms for sterile neutrino with collider signatures, the direct production channels at the e^+e^- , ep colliders and indirect production through heavy particles decay are considered. Our results will provide complementary tests for the possible see-saw and radiative generated mass probe of sterile neutrino from GeV to TeV. For the direct production channel at e^+e^- collider, we investigate the W-exchange mechanism at the STCF, the SuperKEKB, the CEPC and the ILC. Numerical results indicate that the canonical cross section is considerable, the sensitivity for active-sterile mixing $|U_{\ell N}|^2$ is given at the 95% confidence level. According to our estimation, the lower sensitivity limit can reach 10^{-5} in $0.3 - 2$ GeV region for lower energy e^+e^- collider, *e.g.*, the STCF and the SuperKEKB; extended to 10^{-7} in electroweak energy mass region for high energy collider, *e.g.*, the CEPC and the ILC. For the direct production channel at ep collider, we explore the γ - W^* fusion mechanism at the LHeC using proton bremsstrahlung. The canonical production cross section for $e^-\gamma \rightarrow NW^-$ process can reach tens fb if we probe a electroweak energy mass scale sterile neutrino, the low sensitivity limit of $|U_{eN}|^2$ will reach 10^{-4} at this mass region. Besides, the Dirac or Majorana nature of the sterile neutrino can be tested via the sign of single lepton in $N \rightarrow \ell jj$ decay.

We also studied the indirect production channels via hadron (meson and baryon) and Higgs decay. For heavy meson, we proposed a new search method for sterile neutrino via kink structure in lepton energy spectrum of B-meson semileptonic decay. For heavy baryon, we explore the four-body decay of $\Lambda_c, \Xi_c, \Xi_{cc}$ and Λ_b . Numerical results show that the $|U_{\ell N}|^2$ are sensitive slightly above the $\mu\pi$ threshold. Considering the yields of heavy baryon is large at the LHCb, the constrain plane is given in this region. For Higgs decay, we investigate the Higgs $\rightarrow W\mu\mu\pi$ process with relative clear signal, the

constrain of mixing parameter is also given. The low sensitivity limits of $|U_{\ell N}|^2$ versus sterile neutrino mass from channels of this article and present experimental limits are given in FIG.12 - 13.

Acknowledgments The author would like to thank Jingyi Xu for useful discussion of detection efficiency at the LHC. The work of Cong-Feng Qiao is supported in part by the National Key Research and Development Program of China under Contracts No. 2020YFA0406400, and the National Natural Science Foundation of China (NSFC) under the Grants No. 11975236, No. 11635009, No. 12047553, and No. 12235008. The work of Bingwei Long is supported by the National Natural Science Foundation of China (NSFC) under Grants No. 12275185 and No. 12335002.

-
- [1] P. Minkowski, Phys. Lett. B **67**, 421-428 (1977) doi:10.1016/0370-2693(77)90435-X
 - [2] R. N. Mohapatra and G. Senjanovic, Phys. Rev. Lett. **44**, 912 (1980) doi:10.1103/PhysRevLett.44.912
 - [3] K. S. Babu and E. Ma, Mod. Phys. Lett. A **4**, 1975 (1989) doi:10.1142/S0217732389002239
 - [4] N. Arkani-Hamed, S. Dimopoulos, G. R. Dvali and J. March-Russell, Phys. Rev. D **65**, 024032 (2001) doi:10.1103/PhysRevD.65.024032 [arXiv:hep-ph/9811448 [hep-ph]].
 - [5] F. F. Deppisch, P. S. Bhupal Dev and A. Pilaftsis, New J. Phys. **17**, no.7, 075019 (2015) doi:10.1088/1367-2630/17/7/075019 [arXiv:1502.06541 [hep-ph]].
 - [6] M. Doi, T. Kotani and E. Takasugi, Prog. Theor. Phys. Suppl. **83**, 1 (1985) doi:10.1143/PTPS.83.1
 - [7] M. Galeazzi, F. Fontanelli, F. Gatti and S. Vitale, Phys. Rev. Lett. **86**, 1978-1981 (2001) doi:10.1103/PhysRevLett.86.1978
 - [8] K. H. Hiddeemann, H. Daniel and O. Schwentker, J. Phys. G **21**, 639-650 (1995) doi:10.1088/0954-3899/21/5/008

- [9] E. Holzschuh, W. Kundig, L. Palermo, H. Stussi and P. Wenk, Phys. Lett. B **451**, 247-255 (1999) doi:10.1016/S0370-2693(99)00200-2
- [10] E. Holzschuh, L. Palermo, H. Stussi and P. Wenk, Phys. Lett. B **482**, 1-9 (2000) doi:10.1016/S0370-2693(00)00476-7
- [11] J. Deutsch, M. Lebrun and R. Prieels, Nucl. Phys. A **518**, 149-155 (1990) doi:10.1016/0375-9474(90)90541-S
- [12] D. I. Britton, S. Ahmad, D. A. Bryman, R. A. Burnbam, E. T. H. Clifford, P. Kitching, Y. Kuno, J. A. Macdonald, T. Numao and A. Olin, *et al.* Phys. Rev. Lett. **68**, 3000-3003 (1992) doi:10.1103/PhysRevLett.68.3000
- [13] T. Yamazaki, T. Ishikawa, Y. Akiba, M. Iwasaki, K. H. Tanaka, S. Ohtake, H. Tamura, M. Nakajima, T. Yamanaka and I. Arai, *et al.* Conf. Proc. C **840719**, 262 (1984)
- [14] D. A. Bryman and R. Shrock, Phys. Rev. D **100**, no.5, 053006 (2019) doi:10.1103/PhysRevD.100.053006 [arXiv:1904.06787 [hep-ph]].
- [15] D. A. Bryman and R. Shrock, Phys. Rev. D **100**, 073011 (2019) doi:10.1103/PhysRevD.100.073011 [arXiv:1909.11198 [hep-ph]].
- [16] P. Rubin *et al.* [CLEO], Phys. Rev. D **82**, 092007 (2010) doi:10.1103/PhysRevD.82.092007 [arXiv:1009.1606 [hep-ex]].
- [17] O. Seon *et al.* [BELLE], Phys. Rev. D **84**, 071106 (2011) doi:10.1103/PhysRevD.84.071106 [arXiv:1107.0642 [hep-ex]].
- [18] R. Aaij *et al.* [LHCb], Phys. Rev. Lett. **112**, no.13, 131802 (2014) doi:10.1103/PhysRevLett.112.131802 [arXiv:1401.5361 [hep-ex]].
- [19] M. Ablikim *et al.* [BESIII], Phys. Rev. D **99**, no.11, 112002 (2019) doi:10.1103/PhysRevD.99.112002 [arXiv:1902.02450 [hep-ex]].
- [20] O. Adriani *et al.* [L3], Phys. Lett. B **295**, 371-382 (1992) doi:10.1016/0370-2693(92)91579-X
- [21] P. Abreu *et al.* [DELPHI], Z. Phys. C **74**, 57-71 (1997) [erratum: Z. Phys. C **75**, 580 (1997)] doi:10.1007/s002880050370
- [22] G. Aad *et al.* [ATLAS], Phys. Rev. Lett. **131**, no.6, 061803 (2023)

- doi:10.1103/PhysRevLett.131.061803 [arXiv:2204.11988 [hep-ex]].
- [23] S. Chatrchyan *et al.* [CMS], Phys. Lett. B **717**, 109-128 (2012) doi:10.1016/j.physletb.2012.09.012 [arXiv:1207.6079 [hep-ex]].
- [24] V. Khachatryan *et al.* [CMS], Phys. Lett. B **748**, 144-166 (2015) doi:10.1016/j.physletb.2015.06.070 [arXiv:1501.05566 [hep-ex]].
- [25] G. Aad *et al.* [ATLAS], JHEP **07**, 162 (2015) doi:10.1007/JHEP07(2015)162 [arXiv:1506.06020 [hep-ex]].
- [26] G. Aad *et al.* [ATLAS], Eur. Phys. J. C **72**, 2056 (2012) doi:10.1140/epjc/s10052-012-2056-4 [arXiv:1203.5420 [hep-ex]].
- [27] A. M. Sirunyan *et al.* [CMS], Phys. Rev. Lett. **120**, no.22, 221801 (2018) doi:10.1103/PhysRevLett.120.221801 [arXiv:1802.02965 [hep-ex]].
- [28] B. Pontecorvo, Sov. Phys. JETP **6**, 429 (1957)
- [29] Z. Maki, M. Nakagawa and S. Sakata, Prog. Theor. Phys. **28**, 870-880 (1962) doi:10.1143/PTP.28.870
- [30] S. Antusch, E. Cazzato and O. Fischer, Int. J. Mod. Phys. A **32**, no.14, 1750078 (2017) doi:10.1142/S0217751X17500786 [arXiv:1612.02728 [hep-ph]].
- [31] G. Zhang and B. Q. Ma, Phys. Rev. D **103**, no.3, 033004 (2021) doi:10.1103/PhysRevD.103.033004 [arXiv:2101.05566 [hep-ph]].
- [32] A. Atre, T. Han, S. Pascoli and B. Zhang, JHEP **05**, 030 (2009) doi:10.1088/1126-6708/2009/05/030 [arXiv:0901.3589 [hep-ph]].
- [33] J. N. Ding, Q. Qin and F. S. Yu, Eur. Phys. J. C **79**, no.9, 766 (2019) doi:10.1140/epjc/s10052-019-7277-3 [arXiv:1903.02570 [hep-ph]].
- [34] M. Gluck, C. Pisano and E. Reya, Phys. Lett. B **540**, 75-80 (2002) doi:10.1016/S0370-2693(02)02125-1 [arXiv:hep-ph/0206126 [hep-ph]].
- [35] R. E. Shrock, Phys. Lett. B **96**, 159-164 (1980) doi:10.1016/0370-2693(80)90235-X
- [36] M. Daum, G. H. Eaton, R. Frosch, H. Hirschmann, J. McCulloch, R. C. Minehart and E. Steiner, Phys. Lett. B **74**, 126-129 (1978) doi:10.1016/0370-2693(78)90077-1
- [37] E. Kou *et al.* [Belle-II], PTEP **2019**, no.12, 123C01 (2019) [erratum: PTEP **2020**, no.2,

- 029201 (2020)] doi:10.1093/ptep/ptz106 [arXiv:1808.10567 [hep-ex]].
- [38] A. Ali, A. V. Borisov and N. B. Zamorin, Eur. Phys. J. C **21**, 123-132 (2001) doi:10.1007/s100520100702 [arXiv:hep-ph/0104123 [hep-ph]].
- [39] C. Dib, V. Gribov, S. Kovalenko and I. Schmidt, Phys. Lett. B **493**, 82-87 (2000) doi:10.1016/S0370-2693(00)01134-5 [arXiv:hep-ph/0006277 [hep-ph]].
- [40] R. L. Workman *et al.* [Particle Data Group], PTEP **2022**, 083C01 (2022) doi:10.1093/ptep/ptac097
- [41] M. T. Prim *et al.* [Belle], Phys. Rev. D **101**, no.3, 032007 (2020) doi:10.1103/PhysRevD.101.032007 [arXiv:1911.03186 [hep-ex]].
- [42] C. H. Chang, C. D. Lu, G. L. Wang and H. S. Zong, Phys. Rev. D **60**, 114013 (1999) doi:10.1103/PhysRevD.60.114013 [arXiv:hep-ph/9904471 [hep-ph]].
- [43] J. Mejia-Guisao, D. Milanes, N. Quintero and J. D. Ruiz-Alvarez, Phys. Rev. D **96**, no.1, 015039 (2017) doi:10.1103/PhysRevD.96.015039 [arXiv:1705.10606 [hep-ph]].
- [44] Y. J. Shi, W. Wang and Z. X. Zhao, Eur. Phys. J. C **80**, no.6, 568 (2020) doi:10.1140/epjc/s10052-020-8096-2 [arXiv:1902.01092 [hep-ph]].
- [45] Y. J. Shi, Y. Xing and Z. X. Zhao, Eur. Phys. J. C **79**, no.6, 501 (2019) doi:10.1140/epjc/s10052-019-7014-y [arXiv:1903.03921 [hep-ph]].
- [46] K. Azizi, Y. Sarac and H. Sundu, Eur. Phys. J. A **48**, 2 (2012) doi:10.1140/epja/i2012-12002-1 [arXiv:1107.5925 [hep-ph]].
- [47] S. Acharya *et al.* [ALICE], Phys. Rev. D **105**, no.1, L011103 (2022) doi:10.1103/PhysRevD.105.L011103 [arXiv:2105.06335 [nucl-ex]].
- [48] R. Aaij *et al.* [LHCb], Phys. Rev. D **100**, no.3, 031102 (2019) doi:10.1103/PhysRevD.100.031102 [arXiv:1902.06794 [hep-ex]].
- [49] R. Aaij *et al.* [LHCb], JHEP **03**, 159 (2016) [erratum: JHEP **09**, 013 (2016); erratum: JHEP **05**, 074 (2017)] doi:10.1007/JHEP03(2016)159 [arXiv:1510.01707 [hep-ex]].
- [50] R. Aaij *et al.* [LHCb], Phys. Rev. Lett. **118**, no.5, 052002 (2017) [erratum: Phys. Rev. Lett. **119**, no.16, 169901 (2017)] doi:10.1103/PhysRevLett.118.052002 [arXiv:1612.05140 [hep-ex]].

- [51] S. Acharya *et al.* [ALICE], Phys. Rev. Lett. **127**, no.27, 272001 (2021) doi:10.1103/PhysRevLett.127.272001 [arXiv:2105.05187 [nucl-ex]].
- [52] R. Aaij *et al.* [LHCb], Chin. Phys. C **44**, no.2, 022001 (2020) doi:10.1088/1674-1137/44/2/022001 [arXiv:1910.11316 [hep-ex]].
- [53] T. Gutsche, M. A. Ivanov, J. G. Körner, V. E. Lyubovitskij and Z. Tyulemissov, Phys. Rev. D **100**, no.11, 114037 (2019) doi:10.1103/PhysRevD.100.114037 [arXiv:1911.10785 [hep-ph]].
- [54] R. Aaij *et al.* [LHCb], Phys. Rev. D **102**, no.7, 071101 (2020) doi:10.1103/PhysRevD.102.071101 [arXiv:2007.12096 [hep-ex]].
- [55] P. S. Bhupal Dev, R. Franceschini and R. N. Mohapatra, Phys. Rev. D **86**, 093010 (2012) doi:10.1103/PhysRevD.86.093010 [arXiv:1207.2756 [hep-ph]].
- [56] A. Das, Y. Gao and T. Kamon, Eur. Phys. J. C **79**, no.5, 424 (2019) doi:10.1140/epjc/s10052-019-6937-7 [arXiv:1704.00881 [hep-ph]].
- [57] H. O. Back, M. Belata, A. de Bari, T. Beau, A. de Bellefon, G. Bellini, J. Benziger, S. Bonetti, C. Buck and B. Caccianiga, *et al.* JETP Lett. **78**, 261-266 (2003) doi:10.1134/1.1625721
- [58] C. Hagner, M. Altmann, F. von Feilitzsch, L. Oberauer, Y. Declais and E. Kajfasz, Phys. Rev. D **52**, 1343-1352 (1995) doi:10.1103/PhysRevD.52.1343
- [59] G. Bernardi, G. Carugno, J. Chauveau, F. Dicarolo, M. Dris, J. Dumarchez, M. Ferro-Luzzi, J. M. Levy, D. Lukas and J. M. Perreau, *et al.* Phys. Lett. B **203**, 332-334 (1988) doi:10.1016/0370-2693(88)90563-1
- [60] J. Badier *et al.* [NA3], Z. Phys. C **31**, 21 (1986) doi:10.1007/BF01559588
- [61] F. Bergsma *et al.* [CHARM], Phys. Lett. B **166**, 473-478 (1986) doi:10.1016/0370-2693(86)91601-1
- [62] D. Liventsev *et al.* [Belle], Phys. Rev. D **87**, no.7, 071102 (2013) [erratum: Phys. Rev. D **95**, no.9, 099903 (2017)] doi:10.1103/PhysRevD.87.071102 [arXiv:1301.1105 [hep-ex]].
- [63] A. Kusenko, S. Pascoli and D. Semikoz, JHEP **11**, 028 (2005) doi:10.1088/1126-6708/2005/11/028 [arXiv:hep-ph/0405198 [hep-ph]].

- [64] P. Vilain *et al.* [CHARM II], Phys. Lett. B **343**, 453-458 (1995) doi:10.1016/0370-2693(94)01422-9
- [65] A. M. Cooper-Sarkar *et al.* [WA66], Phys. Lett. B **160**, 207-211 (1985) doi:10.1016/0370-2693(85)91493-5
- [66] E. Gallas *et al.* [FMMF], Phys. Rev. D **52**, 6-14 (1995) doi:10.1103/PhysRevD.52.6
- [67] A. Vaitaitis *et al.* [NuTeV and E815], Phys. Rev. Lett. **83**, 4943-4946 (1999) doi:10.1103/PhysRevLett.83.4943 [arXiv:hep-ex/9908011 [hep-ex]].